Electrostatics Explains the Shift in VDAC Gating with Salt Activity Gradient

Victor Levadny,*† Marco Colombini,‡ Xiao Xian Li,‡ and Vicente M. Aguilella*
*Departamento de Ciencias Experimentales, Universidad Jaume I, 12080 Castellón, Spain; †The Scientific Council for Cybernetics, Russian Academy of Sciences, 333117 Moscow, Russia, and ‡Department of Biology, University of Maryland, College Park, Maryland 20742 USA

ABSTRACT We have analyzed voltage-dependent anion-selective channel (VDAC) gating on the assumption that the states occupied by the channel are determined mainly by their electrostatic energy. The voltage dependence of VDAC gating both in the presence and in the absence of a salt activity gradient was explained just by invoking electrostatic interactions. A model describing this energy in the main VDAC states has been developed. On the basis of the model, we have considered how external factors cause the redistribution of the channels among their conformational states. We propose that there is a difference in the electrostatic interaction between the voltage sensor and fixed charge within the channel when the former is located in the *cis* side of membrane as opposed to the *trans*. This could be the main cause of the shift in the probability curve. The theory describes satisfactorily the experimental data (Zizi et al., *Biophys. J.* 1998. 75:704–713) and explains some peculiarities of VDAC gating. The asymmetry of the probability curve was related to the apparent location of the VDAC voltage sensor in the open state. By analyzing published experimental data, we concluded that this apparent location is influenced by the diffusion potential. Also discussed is the possibility that VDAC gating at high voltage may be better described by assuming that the mobile charge consists of two parts that have to overcome different energetic barriers in the channel-closing process.

INTRODUCTION

The voltage-dependent anion-selective channel (VDAC) is a voltage-gated charged channel from the mitochondrial outer membrane. Purified from mitochondria and placed into a phospholipid membrane, it exhibits two main conductive levels (connected through the gating process): a high-conductance state (the open state), for zero or very low transmembrane voltages; and low-conductance states achieved at both positive and negative applied transmembrane voltage (Colombini et al., 1996). The reversal potential measurements of point mutants (Peng et al., 1992) have shown that the apparent VDAC charge in the open state is positive, but it is negative in the closed state. The gating mechanism for VDAC is still under discussion, but a great deal of evidence indicates that some charged regions of the channel (called the "voltage sensor") move across the membrane during the gating process (Colombini et al., 1996; Song et al., 1998). This mechanism can be represented as follows. VDAC has a positively charged, mobile voltage-sensing domain, which can be either inside or outside VDAC. Its displacement, change of channel radius, and concomitant inversion in ion selectivity are the main events in the gating process. The mobile voltage-sensing domain is located inside VDAC in the open state, but it is located somewhere outside in the closed state. Moreover, there are two different closed states: *trans*-closed (or "closed-N" following the notation of Zizi et al., 1998), when the voltage-sensing domain is in the *trans* solution, and *cis*-closed (or "closed-P"), when it is in the *cis* solution.

The charge of the sensor accounts for the voltage dependence of the VDAC conductivity. It contains both positive and negative charges, but its net charge is positive (Thomas et al., 1993; Ermishkin and Mirzabekov, 1990).

The dependence of the channel's open-state probability on the applied voltage V is one of the main characteristics of VDAC gating. In the absence of a salt activity gradient, the maximum open-state probability corresponds to very low voltages, $V \sim 0$, but a salt activity gradient induces a shift in the voltage needed to open the channel. The gradient favors channel closure for one gating process (negative) and opening for the other. Generally speaking, the probability curve of VDAC obtained in experiments shows a few important features (Zizi et al., 1998): it is bell-shaped, centered around zero applied voltage in the absence of a salt activity gradient; its peak is shifted to the region of negative voltages in the presence of a salt activity gradient; the steepness of the voltage dependence is not the same for voltages greater and lower than the peak voltage; and the asymmetry of the probability curve depends on the type of salt. In particular, VDAC channels placed in charged soybean phospholipids show a symmetrical gating processes, but when placed in pure neutral lipids, the two gating processes display a slightly different voltage dependence (Zizi et al., 1998).

The shift of the open-state probability curve in the presence of an activity gradient has been explained by invoking a transfer of kinetic energy from salt ions to the mobile

Submitted August 7, 2001, and accepted for publication January 8, 2002.
Address reprint requests to Vicente M. Aguilella, Departamento de Ciencias Experimentales, Universidad Jaume I, AP 220, 12080 Castellón, Spain. Tel.: 34-964-728045; Fax: 34-964-728066; E-mail: aguilell@uji.es.

0006-3495/02/04/1773/11 $2.00

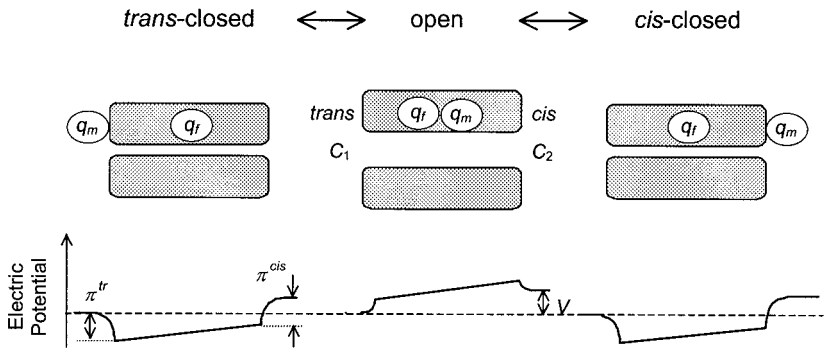

FIGURE 1 Sketch of the three states among which channels redistribute. An illustration of the total electric potential profile (which includes a positive applied transmembrane potential and potentials caused by charges within VDAC's pore) is shown. $q_f < 0$ is the fixed charge within the channel, and $q_m > 0$ is the net charge of the voltage sensor (the mobile charge); $|q_m| > |q_f|$ for VDAC, so that the net charge in the channel open state is positive. See main text for details.

domain (Zizi et al., 1998). Collisions of ions with the voltage-sensor region on the protein wall forming the VDAC pore as these ions move according to their electrochemical gradient was proposed to impart net kinetic energy to this mobile region, resulting in a bias in the probability of the channel being in a particular conformational state. However, this approach does not explain other features of the gating in presence of the activity gradient. Here we propose a complementary explanation based only on electrostatic interactions and show that some additional useful information can be extracted from the voltage dependence of the channel's open-state probability. In general, there are a lot of electrostatic interactions that influence the gating process. We show here that it is possible to make a simple model based only on a few main interactions. In particular, the interaction of the charged voltage sensor with the externally applied field and with the fixed charge of the channel determines the main characteristics of the gating process. We describe VDAC as a three-state system, i.e., it is assumed that the channel may be in one of these three main states: open state, when the mobile sensor is inside the channel; *trans*-closed state, when it is facing the *trans* solution; and *cis*-closed state, when it is facing the *cis* solution (Fig. 1). Then, by modeling the electrostatic interactions existing in the system, we analyze the distribution of the channels among these states in the absence and in the presence of a salt activity gradient. We show that the initial unequal occupancy of the *trans*-closed state and *cis*-closed state at zero applied voltage and in the presence of a salt activity gradient is the cause of the shift in the open-state probability curve. Moreover, this difference in occupancy is, in turn, the result of different electrostatic interactions of the voltage sensor with the channel's fixed charge, when the former is on the *cis* side of membrane as opposed to the *trans* side. The model developed explains not only such basic characteristics of VDAC gating as the shift in the presence of an activity gradient, but also other minor details such as the asymmetry in the probability curve and its behavior at high applied voltages.

THEORY

The model of VDAC charge distribution

VDAC contains a number of charged residues that line the aqueous pore (Colombini et al., 1996). Generally, VDAC can undergo conformational changes under the influence of external factors such as the applied electric field and concentrations of constituents in surrounding solutions. Some of these rearrangements result in easily observable effects (such as channel closing and opening), but others produce no easily detectable effects (Rostovtseva et al., 2000). In most cases, the structural rearrangements change the channel charge distribution. In this connection, all charged residues within the channel can be divided into two groups: a group of relatively immobile "fixed" residues, located always inside the channel (their net charge, hereafter denoted as channel fixed charge q_f, is negative); and a group of relatively mobile residues located inside the channel in the open state and outside the channel in the closed state (their net charge, hereafter denoted as channel mobile charge q_m, is positive). The mobile charge is considered to be the same as the charge on the voltage sensor. To simplify the mathematical treatment, we introduce the apparent axial location of this mobile charge as

$$x_m = -1 + \frac{1}{q_m} \sum_j q_j (x_j + 1)$$

(see its formal determination below in Eq. 4). q_j and x_j denote the charge of the jth residue and its axial coordinate, respectively (both dimensionless, i.e., q_j is in e units; x in L units where $2L$ is the length of the channel, and x origin is at the channel midpoint); the sum extends over all mobile

TABLE 1 List of symbols

C_1	Activity on *trans* side
C_2	Activity on *cis* side
q_m	Charge of mobile voltage-sensing domain in VDAC
q_f	Fixed charge within the pore of VDAC
V	Transmembrane potential of the applied electric field in *cis-trans*
V_{max}	Value of the applied transmembrane voltage that gives maximum probability P_{max}
ΔV_{max}	Shift of V_{max} due to salt gradient, $C_1 \neq C_2$
π^{cis}, π^{tr}	Donnan potentials at *cis* and *trans* sides of the membrane in the closed state of VDAC, respectively
E^i	Energy of *i*th state (in *kT* units)
P^i	Probability of *i*th state
P	Relative probability open versus closed
P_0	$P(V = 0)$ in the absence of salt activity gradient
P_{max}	$P(V_{max})$
N	Total number of channels in the system
N^i	Number of channels in *i*th state, where *i* = open (op), *cis*-closed (cis), *trans*-closed (tr)
α	Constant dependent on the channel radius and length
x	Axial coordinate
x_m	Apparent axial location of mobile charge q_m

All magnitudes are dimensionless.

charge residues (see Table 1). By assuming that *cis*-closed state corresponds to the location of all voltage sensor charges at $x_j = 1$, one obtains $x_m \approx +1$ in this state. A similar statement holds for *trans*-closed state at $x_j = -1$; it leads to $x_m \approx -1$. In the open state, charged residues are located inside the channel, i.e., in this state $-1 < x_j < 1$ so that $-1 < x_m < 1$. $x_m = 0$ corresponds to an apparent location of q_m exactly in the channel midpoint for the open state of VDAC. Hence, the deviation of x_m from 0 describes actually the displacement of apparent mobile charge from the channel midpoint. Any variations of external conditions that result in a change of the local electric field will affect q_j, thus changing x_j and therefore x_m.

Reversal potential measurements (Peng et al., 1992) have demonstrated that VDAC's fixed charge, q_f, is negative, but the mobile charge is positive. It is worth noting that this description of mobile charges is the simplest one. Generally, mobile charges can be described by a few groups, each one having its own energy barrier. We will show below that the representation of the channel's mobile charges by at least two charged groups gives a better description of VDAC gating at high applied voltages.

The probabilities of VDAC states

Let us consider N VDAC channels reconstituted into a membrane bathed by an aqueous electrolyte solution with activities C_1 on the *trans* side and C_2 on the *cis*. The bulk of the *trans* solution is taken as virtual ground when an external electrical field is applied. In accordance with the above discussed charge model, we describe here the overall channel charge as consisting of two parts: a negative fixed charge, $q_f < 0$, located always inside the channel; and a positive mobile charge, $q_m > 0$, located inside the channel in the open state and outside the channel in the closed state. This modeling of channel charges gives the simplest description of VDAC as a three-state system, i.e., the channel can be in one of these three different states: open state, when the mobile charge q_m is inside the channel; *trans*-closed state, when the mobile charge q_m faces the *trans* solution; and *cis*-closed state, when the mobile charge q_m faces the *cis* solution (Fig. 1).

The probability P^i of the *i*th channel state is determined by its energy E^i

$$P^i = \frac{N^i}{N} = \frac{\exp(-E^i)}{S} = \frac{\exp(-E^i)}{\exp(-E^{cis}) + \exp(-E^{tr}) + \exp(-E^{op})}, \quad (1)$$

where N is the total number of channels in the system; N^i is the number of channels in *i*th state; E^i is the energy of *i*th state (dimensionless, in *kT* units); S is the partition function of the system; and i = open (op), *cis*-closed (cis), or *trans*-closed (tr). A slightly different way to express the propensity of the channel to be in the open state is to define the relative probability to be open versus closed, P,

$$P = \frac{N^{op}}{N^{cis} + N^{tr}} = \frac{P^{op}}{1 - P^{op}} = \frac{\exp(-E^{op})}{\exp(-E^{cis}) + \exp(-E^{tr})}. \quad (2)$$

Because it is straightforward to convert P with P^{op} and mathematical expressions for the former become much simpler, we will derive expressions for P in our treatment.

Each energy term, E^i, includes all interactions involved in VDAC. Some of them are sensitive to external effects such as the applied electric field or the concentration of constituents in the surrounding solutions. But others, e.g., the energy of chemical bonds, are almost insensitive to such effects, in particular, to the applied voltage. Therefore, for our purpose, we divide each energy E^i into two terms: one part, E^i_{elec}, is dependent on the external voltage (i.e., the voltage in its immediate surroundings), which changes with the conformational state of VDAC, and another part, E^i_{other}, includes all other interactions. This is a standard approach. Here we make the assumption that the salt activity gradient influences mainly the electrostatic term. Therefore, in analyzing the voltage dependence of gating, we will consider mainly the interactions of the mobile charge q_m with the externally applied electric field and with the fixed charge q_f.

The probability curve in the absence of a salt activity gradient ($C_1 = C_2$)

Let V be the potential in *cis*-solution associated with the applied electric field. This applied electric field changes the energy, E^i, of each VDAC state and, consequently, the relative probability to be open, P. We will call the function $P(V)$ the open probability. Our aim is to develop the analytical expression for $P(V)$. For that, we have to consider first of all the electrostatic interaction of the mobile charge, q_m, with the applied electric field in each conformational state of VDAC mentioned above.

The interaction of the voltage sensor with the externally applied field depends on the location of its charged residues and their dielectric environment. The electric potential inside the channel near the *trans* entrance is nearly zero, and it is close to V near the *cis* entrance. Similar assumptions have been used in the modeling of VDAC reversal potential in the open state, provided end-effects are taken into account (Zambrowicz and Colombini, 1993; Levadny and Aguilella, 2001). Because the interaction energy of the externally applied field with the voltage sensor depends on sensor location, the level is lower if the sensor is located closer to *trans* entrance than to *cis* one. From the general expression for electrostatic energy

$$E_{el} = \sum_j q_j v(x_j)$$

(where $v(x)$ is the potential profile of the externally applied field), by assuming that the applied electric potential profile inside VDAC is linear, i.e., $v(x) = (x + 1)V/2$, one can represent the interaction energy of the mobile charges (of the sensor) with the applied electric field in the open state as

$$E_{el}^{op} = \sum_j q_j v(x_j) = q_m(x_m + 1)V/2, \qquad (3)$$

where the apparent location of q_m is determined by the distribution of mobile charges and by the applied electric field profile in the open state,

$$x_m + 1 = \frac{2}{q_m V}\sum_j q_j v(x_j) = \frac{1}{q_m}\sum_j q_j(x_j + 1). \qquad (4)$$

In our approach, x_m describes the location of charged residues of the mobile sensor. But, generally speaking, as seen from Eqs. 3 and 4, x_m has a more general meaning. x_m may change as a result of charge displacement (already discussed) and as a result of variation of the electric field near each charge residue without any physical displacement of the charged group (Song et al., 1998).

As for closed states, the description of their electrostatic energies is obvious (see equations below). The energies of the open (E^{op}), and closed (E^{tr}, E^{cis}) states in the absence of a salt activity gradient ($C_1 = C_2$) are

$$E^{op} = (x_m + 1)q_m V/2 + E_{other}^{op}, \qquad (5a)$$

$$E^{cis} = q_m V + E_{other}^{cl}, \qquad (5b)$$

$$E^{tr} = E_{other}^{cl}. \qquad (5c)$$

All potentials and charges are dimensionless, i.e., in kT/e and e units, respectively. The terms E_{other}^{i} correspond to interactions that do not influence the voltage dependence of the probability curves. They include the energy of hydrogen-bond breakage during channel closure (Colombini et al., 1996), the interaction energy of fixed charges with the applied electric field, and the interaction of q_m with q_f. For simplicity, we assume that the interactions that do not influence the voltage dependence are the same for both closed states. As it is known, channel opening is 1000 times faster than the channel closure (Colombini, 1979). This fact allows one to estimate the difference between E_{other}^{i} in different states as $E_{other}^{cl} - E_{other}^{op} \approx 7$ (kT units).

By combining Eq. 2 with Eqs. 5, one gets the relative probability of the channel open state,

$$P = P_0\frac{\exp(-x_m q_m V/2)}{\cosh(q_m V/2)}, \qquad (6)$$

where P_0 is the probability to be open at $V = 0$, and, generally, it is not equal to the maximum probability, P_{max}, which is

$$P_{max} = P_0(1 - x_m)^{(1-x_m)/2}(1 + x_m)^{(1+x_m)/2}, \qquad (7)$$

and it is reached at $V_{max} = \ln[(1 - x_m)/(1 + x_m)]/q_m$. At $x_m \cong 0$, $V_0 \cong 0$, and $P_{max} \cong P_0$. Then the expression for P becomes

$$P = \frac{P_{max}}{\cosh(q_m V/2)}. \qquad (8)$$

The probability curve in the presence of a salt activity gradient ($C_1 < C_2$)

The terms E_{other}^{i} in Eqs. 5 contain the electrostatic interaction between the mobile charged domain and the channel fixed charge as well as other contributions. This interaction does not have a V-dependent influence on the relative probability P in the absence of a salt activity gradient. This is the reason why we did not consider explicitly this interaction above. However, in the presence of a salt activity gradient, $C_1 < C_2$ (*trans* < *cis*), the interaction of these charges in the *cis*-closed state differs significantly from the same in the *trans*-closed state. The physical origin of the difference is obvious: in *cis*-closed state the voltage sensor interacts with fixed channel charge through the solution in the *cis*-half of the channel, where the average concentration is greater than

that in the *trans*-half of the channel. Therefore, the mobile charge is more screened in the *cis*-closed state than in the *trans*-closed state. The electrostatic interaction between charges is weaker in the former case. Taking into account that $q_m q_f < 0$, it means that the *trans*-closed state becomes energetically favorable in comparison with the *cis*-closed state in the presence of a salt activity gradient.

So, the interaction of q_m with q_f in the closed states has to be considered explicitly if there is a salt activity gradient. The potential φ^i of the electric field created by fixed charges in *i*th (*trans*- or *cis*-) solutions can be estimated, e.g., from the common solution of the Poisson–Boltzmann equation for a charged cylindrical pore (see, e.g., Sørensen and Koefoed, 1974), which implicitly assumes a homogeneous distribution of fixed charge along the pore wall,

$$\varphi^i = \alpha \frac{q_f}{C_i}. \tag{9}$$

Parameter α is determined by the channel size (radius R and length $2L$), and, for closed VDAC in a 1:1 electrolyte solution, it is $\alpha = 0.26/R^2L$ nm$^3 \approx 0.04$. In summary, the corresponding expressions to Eqs. 5 are now

$$E^{op} = (x_m + 1)q_m V/2 + E^{op}_{other}, \tag{10a}$$

$$E^{cis} = q_m\left(V + q_f \frac{\alpha}{C_2}\right) + E^{cl}_{other}, \tag{10b}$$

$$E^{tr} = q_m q_f \frac{\alpha}{C_1} + E^{cl}_{other}. \tag{10c}$$

From Eq. 2 and Eqs. 10, one gets

$$P(V) = A\,\frac{\exp[x_m q_m(\Delta V_{max} - V)/2]}{\cosh[q_m(\Delta V_{max} - V)/2]}, \tag{11}$$

where ΔV_{max} is the shift of the applied transmembrane voltage that gives maximum probability, P_{max}, for the open state,

$$\Delta V_{max} = \alpha q_f\left(\frac{1}{C_1} - \frac{1}{C_2}\right). \tag{12}$$

As can be seen, Eq. 11 becomes Eq. 6 when $C_1 = C_2$. A is a constant given by

$$A = P_0\,\frac{\cosh[q_m \Delta V_{max}/2]}{\exp[q_m(2x_m - 1)\Delta V_{max}/2]}. \tag{13}$$

This can also be interpreted in the framework of the Donnan approach, assuming that fixed charge in the channel q_f gives rise to Donnan potentials π^{cis} and π^{tr} at the *cis* and *trans* sides of the membrane, respectively. Moreover, they are not equal in the presence of a salt activity gradient (see Fig. 1). Taking into account that $\pi^i \cong \alpha q_f/C_i$ (this approximation of the Donnan potential is valid when the equivalent fixed-charge volume density in the channel is lower or comparable to bulk concentration) one can represent ΔV_{max} as

$$\Delta V_{max} = (\pi^{tr} + \pi^{cis}). \tag{14}$$

According to Eq. 14, the shift of the probability curve is given by the difference between the Donnan potentials of the *trans* and *cis* sides in the closed state of VDAC.

The main assumptions made above are: 1) VDAC is represented by a three-state system; 2) the total energy of each state is divided into two terms, one of them dependent on applied voltage and another nondependent; 3) linearity of applied voltage profile is assumed; 4) for simplicity, we describe the real set of voltage sensor charges as a single apparent mobile charge; and 5) we assume that channel fixed charges are homogeneously distributed along the channel wall.

MATERIALS AND METHODS

VDAC channels were isolated from the mitochondrial membranes of a wall-less mutant of the fungus, *Neurospora crassa* (Mannella, 1982). These channel-forming proteins were reconstituted into planar phospholipid membranes made by the monolayer method of Montal and Mueller as described previously (Colombini, 1987). Recordings were made under voltage-clamp conditions. To generate conductance-voltage plots, triangular voltage waves were applied at 5 mHz and the portion of the record in which the channels were reopening was used (The portion in which the channels closed is kinetically delayed). Thus, the results represent a quasi-equilibrium conductance/voltage relationship between the open state and easily accessible closed states. See Zizi et al., 1998, for further details.

RESULTS AND DISCUSSION

The gating in the absence of a salt activity gradient ($C_1 = C_2$)

Figure 2 shows a comparison of the normalized probability of VDAC being in the open state, P^{op}/P^{op}_{max}, calculated according to Eqs. 2 and 6 for two activities of KCl, with values obtained from conductance measurements reported by Zizi et al. (1998). The conductance was measured in a multichannel membrane with equal activities on both sides. The best fit to experimental data was obtained for $q_m = +3.4$ for both activities. As can be seen, despite the simplicity of the model, the agreement between theory and experiment is rather good for almost the whole voltage range. However, the agreement becomes worse in regions of high voltages, and the discrepancy is more pronounced in dilute solutions (see Fig. 2 *b*). This gives an indication that the model used in the derivation of Eq. 6 (based on a single mobile charge) needs modification to explain the probability curve at high voltages. We will later comment on the channel behavior at high voltages (both positive or negative).

In any case, under these conditions of no salt activity gradient, the single mobile-charge model accounts for the two basic features of VDAC gating: the bell shape of the

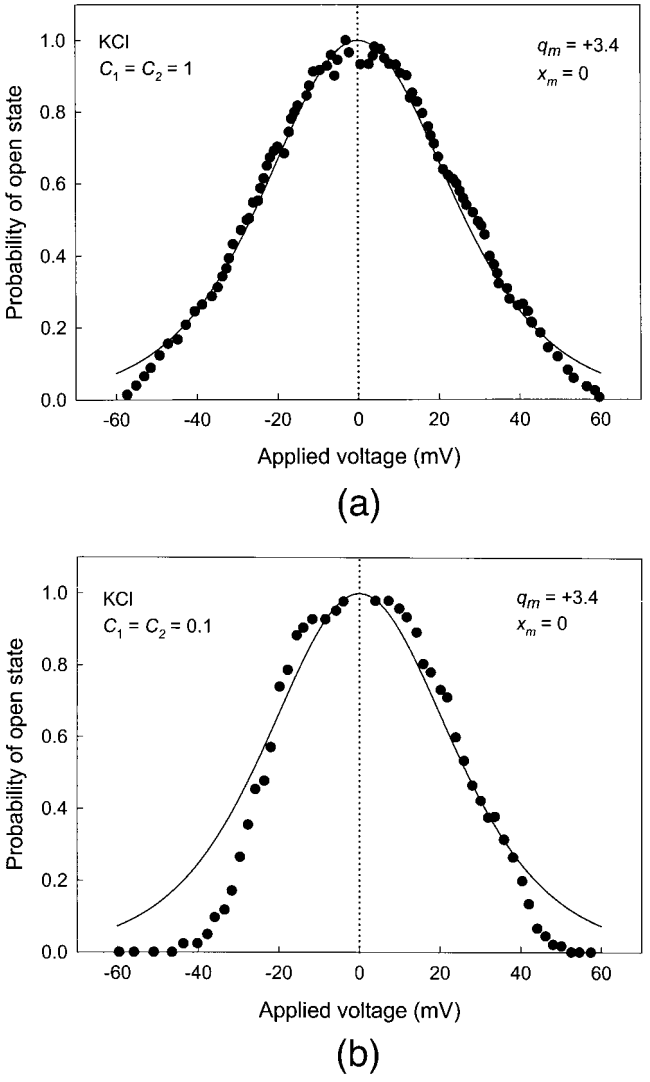

FIGURE 2 The normalized VDAC open probability $P^{op}(V)/P^{op}_{max}$ as a function of transmembrane voltage V without a salt activity gradient in KCl solutions. (*a*) 1 M solution. (*b*) 0.1 M solution. Experimental points (*dots*) are from Zizi et al. (1998). The curves show the theoretical calculations according to Eqs. 2 and 6, by using $q_m \cong +3.4$ and $x_m \cong 0$ as parameter values.

probability curve, i.e., closure observed at both positive and negative potentials with virtually the same steepness of voltage dependence; and maximum open probability achieved at $V_{max} \approx 0$.

VDAC gating in the presence of an applied electric field can be described in the framework of the model developed here. The change in the VDAC gating process (i.e., the change in the relative population of channels in the three states, which determines the probability curve) comes from the difference in the relative electrostatic energies of the states. At $V = 0$, there are a certain number of VDAC channels in each state. An applied electric field induces a redistribution of channels among the states. For example, from Eqs. 5, a positive voltage increases the energy of the open state in comparison with the energy of the *trans*-closed state (similarly, for $V < 0$, the energy of the open state increases in comparison with that of the *cis*-closed state). Thus, a positive voltage causes a new equilibrium to be established by transforming some number of open channels to the *trans*-closed state. However, this voltage also increases the energy of *cis*-closed state in comparison with the open state, causing some number of *cis*-closed channels to transform to the open state. From Eqs. 1 and 5 or from Eqs. 1 and 10, one can obtain that the maximum probability of the channel being in the open state is reached when the energy of both closed states is the same (provided $x_m = 0$). Therefore, the total number of open channels decreases with any nonzero applied voltage. As shown in Fig. 2, this is the case for VDAC. Hence, recalling the physical meaning of parameter x_m in the present model, one can conclude that the apparent location of mobile charge q_m of VDAC in the open state is near its midpoint. This explains both the above-mentioned features of VDAC gating.

Note that the estimated quantity of mobile charge, $q_m = +3.4$, shown in Fig. 2 is of the same order of magnitude as those obtained from selectivity and site-directed mutagenesis experiments. For instance, it was reported from reversal potential measurements that the net charge on the walls forming the pore of yeast VDAC in the open state is $\sim +3e$, and around $-3e$ in the closed state (Peng et al. 1992; Zambrowicz and Colombini, 1993). By assuming that the value of the mobile charge is the difference between the net charge in the open state and the closed state, one gets that apparent VDAC mobile charge is $+6e$. The dual mobile charge model gives an even closer agreement (see discussion below).

The gating in presence of a salt activity gradient ($C_1 < C_2$)

The VDAC probability curve $P(V)$ changes in the presence of a salt gradient (Zizi et al., 1998). The results of the experiments are shown in Fig. 3, together with the predictions of our model. Two sets of experimental measurements are shown: for KBr, and for NaCl. Both have in common the ten-fold salt activity gradient across the membrane (0.06 on *trans* side and 0.6 on *cis* one). The shift in the peak voltage toward negative voltages is approximately the same for both salts (~20 mV). From these experimental data, one can conclude that there are two main effects of the salt gradient on VDAC gating: the maximum of the probability curve shifts to the region of negative applied transmembrane voltage, i.e., $\Delta V_{max} < 0$; and the probability curve becomes asymmetrical.

The solid lines in Fig. 3 are the results of fitting the model to the data by adjusting q_m and x_m. In the case of KBr, best fits were obtained for $q_m \cong 3.2$ and $x_m = -0.3$, whereas, for NaCl, the values were $q_m \cong 3.5$ and $x_m = -0.4$. The model

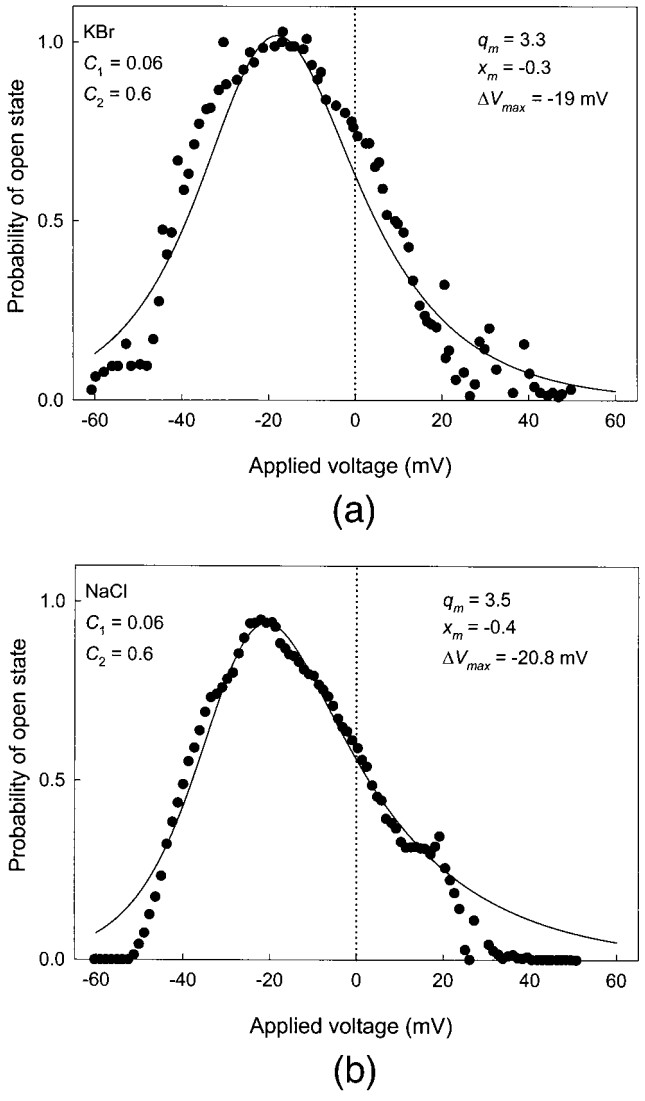

FIGURE 3 The normalized VDAC open probability $P^{op}(V)/P^{op}_{max}$ in the presence of a salt activity gradient (0.06 in *trans* side and 0.6 in *cis* side) for two different salts. (*a*) KBr. (*b*) NaCl. Experimental points (*dots*) are taken from measurements (Zizi et al., 1998). The curves show the theoretical calculations according to Eqs. 2 and 11. The best-fit values of the adjustable parameters are shown on each panel.

describes experimental data reasonably well. Note that, according to the model, the fixed charge q_f determines the sign of ΔV_{max} (see Eq. 12), but the mobile charge q_m and x_m determine the effective gating valence, which is a measure of the steepness of the voltage dependence (see Eq. 11). Actually, $d \ln P/dV \cong -q_m(1 + x_m)/2$ for $V \gg V_{max}$, and $d \ln P/dV \cong q_m(1 - x_m)/2$ for $V \ll V_{max}$.

Let us consider now the physical origin of the shift in the probability curve induced by the salt gradient, in the framework of our model. The main question is: why does the maximum number of open channels correspond to some nonzero transmembrane voltage? As it happens, in the absence of the salt activity gradient, a negative voltage decreases the energy of the open state in comparison with that of the *trans*-closed state, but it increases the energy of open state in comparison with the energy of the *cis*-closed state. In contrast to the case of no activity gradient, the energy of the *cis*-closed state at $V = 0$ is higher than the energy of the *trans*-closed state. This imbalance vanishes at some negative voltage determined by Eq. 12.

The direction of the shift is mainly governed by the sign of the total Donnan potential drop across the channel in its closed state, which is the same as that of the channel fixed charge q_f (see Eq. 14). Because the fixed charge is negative, the maximum open-state probability is achieved at some negative value so that $\Delta V_{max} < 0$. It would be interesting to check whether other voltage-gated channels with a positive fixed charge exhibit an opposite shift of the probability curve.

According to Eq. 12, the absolute value of ΔV_{max} depends essentially on the ion activities of the bathing solutions. Hence, the shifts ΔV_{max} as a function of the activity gradient can be a good test for the model developed here. If the salt activity in the *trans*-solution is kept constant, and the activity in the *cis* side is increased, the Donnan potential on the *cis* side decreases, and the total Donnan potential drop decreases monotonically approaching asymptotically a limiting value π^{tr}. According to Eqs. 12 and 14, the shift ΔV_{max} also approaches a limiting value $\Delta V^*_{max} = \pi^{tr} = \alpha q_f/C_1 \approx 1.4$ (40 mV) (for $x_m = 0$, $R = 1.1$ nm, $2L = 7.5$ nm, $C_1 = 0.06$) as the activity gradient becomes very big. A simple estimation demonstrates that ΔV_{max} reaches 85% of its limiting value ΔV^*_{max} with 10-fold activity ratio. Our model predicts that the variation in $|\Delta V_{max}|$ has to be in the range of 5–10% as the activity ratio is changed from 10- to 20-fold. This prediction was tested experimentally (see Materials and Methods) and the results are shown in Fig. 4. The very small increment in ΔV_{max} (a few mV) when the activity ratio is increased two-fold is in agreement with our theory. Note that this monotonic behavior with an asymptotic limit is not easily distinguishable from that predicted by the kinetic energy transfer mechanism (Zizi et al., 1998).

It is worth noting, however, that we have used here the simplest treatment of the Donnan potential drop, which assumes that the salt activity in the *cis*-solution does not influence the Donnan potential on the *trans*-side. Such an influence can appear for high-activity ratios, where total Donnan potential drop decreases with increases of the activity ratio (Zambrowicz and Colombini, 1993; Levadny and Aguilella, 2001). So one cannot exclude the possibility of a nonmonotonic behavior of $|\Delta V_{max}|$ in the region of high activity ratios.

Asymmetry of the probability curve: salt effects

Here we discuss the deviation of the probability curve from an ideal bell-shape form or, from another point of view, the difference in steepness of the voltage dependence for pos-

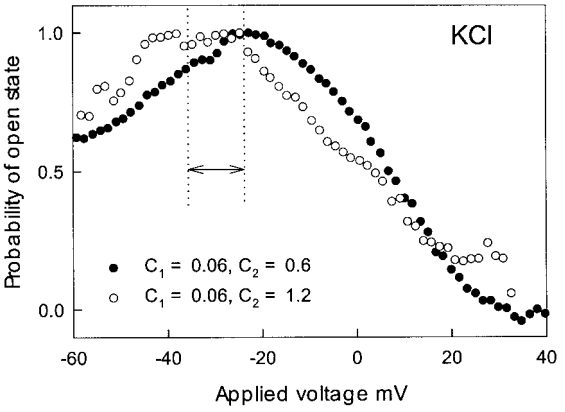

FIGURE 4 The effect of salt activity gradient on the shift ΔV_{max} along the voltage axis. The normalized open probability $P^{op}(V)/P^{op}_{max}$ of VDAC in the presence of two different KCl salt gradients: *filled symbols*, a 10-fold activity ratio (0.06 in *trans* vs. 0.6 in *cis*); *open symbols*, a 20-fold activity ratio (0.06 in *trans* vs. 1.2 in *cis*). See main text for details. The shift in the gating process and limitations in the voltage that could be applied without membrane breakage resulted in closure of only some of the channels at high potentials (triangular wave went up to −70 mV). Nevertheless, the channels that did close reopened as the voltage declined, indicating the location of V_{max}. The double-ended arrow shows the shift of the peak along the voltage axis as the salt gradient was increased from 10- to 20-fold.

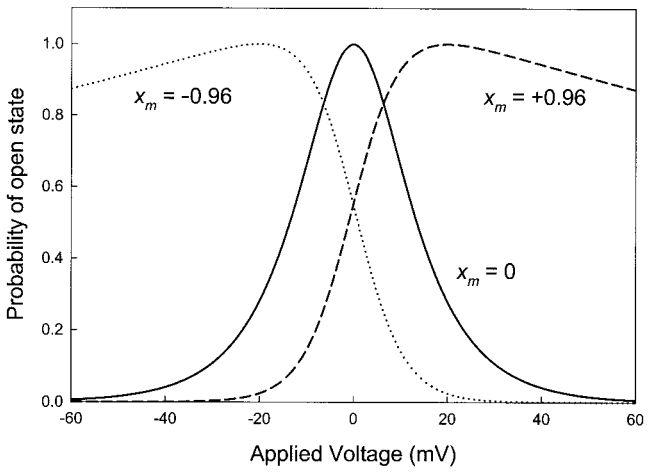

FIGURE 5 The effect of apparent location of mobile charge on the probability curve. The calculated open probability $P^{op}(V)/P^{op}_{max}$ is shown for two limiting cases, $x_m = -0.96$ (apparent location near *cis*-entrance) and $x_m = 0.96$ (apparent location near *trans*-entrance), and for the intermediate situation, $x_m = 0$ (apparent location in channel midpoint).

itive and negative gating processes. We call this characteristic of the system "asymmetry of the probability curve," because, besides a pure geometrical treatment, this phenomenon also reflects an asymmetrical behavior of channel gating. We will show that this feature can be connected with some biophysical characteristics of VDAC.

The following points will be considered: 1) why the probability curve becomes asymmetrical in the presence of an ion activity gradient; 2) why asymmetry is different in different salts; and 3) why VDAC channels in charged phospholipids show a symmetrical gating processes, but in neutral lipids they exhibit asymmetrical gating. As is seen by comparing Fig. 2 with Fig. 3, the probability curves having an almost ideal bell-shape form in experiments with equal salt activities on both sides of the membrane transform into asymmetrical curves in the presence of a salt activity gradient, the asymmetry depending on the type of salt in the bathing solutions. Another experimental fact comes from a comparison of VDAC gating in charged lipid membranes and in neutral ones. In particular, VDAC channels placed in charged soybean phospholipids show symmetrical gating processes, but, when placed in pure neutral lipids, they exhibit asymmetrical gating (Zizi et al. 1998).

To discuss the form of the probability curve, it is necessary first of all to determine the way to measure asymmetry. In our model, x_m can be treated as a quantitative measure of the probability curve asymmetry, as used in Eq. 6. Figure 5 displays the normalized probability curves $P(V)/P_{max}$ for two limiting cases, $x_m = -0.96$ and $x_m = +0.96$, and for one intermediate situation, $x_m = 0$, obtained on the basis of this equation. It is seen that the probability curve with $x_m = 0$ shows the ideal bell-shape form, but deviations of the parameter x_m from 0 result in an asymmetrical probability curve. The disadvantage of this parameter is that it is difficult to get its value directly from experiments, but, using our model, it is possible to connect it to a measurable parameter, the gating valence (see below). Recalling that $x_m = 0$ means a midpoint location of the apparent mobile charge in the channel in the open state, then the appearance of an asymmetrical probability curve could mean displacement of this apparent charge from the center of the channel in this state. Hence, in accordance with our model, the shallower slope (Fig. 5, *dotted line*) of the probability curve in the region $|V| > |V_{max}|$ means that the location of mobile charge is closer to the *trans*-entrance, when the channel is in the open state.

Zizi et al. (1998) reported differences in the values of the positive, n_+, and negative gating valence, n_-, and these are experimental measures of the gating asymmetry. The meaning of these gating valences is the steepness ($d \ln P/dV$) of the probability curve for the positive and negative gating processes. Nevertheless, to discuss the asymmetry, it is useful to introduce a single parameter. We use here the "asymmetry index", defined as the ratio n_-/n_+. From Eq. 6, one can get the relationship of our model parameter x_m with the index $n_-/n_+ \propto (1 - x_m)/(1 + x_m) \approx 1 - 2x_m$.

The experimental index n_-/n_+ varies from 0.8 up to 1.7 depending on the type of salt (n_+ and n_- were taken from Table 2 in Zizi et al., 1998) corresponding to negative values of x_m if $n_-/n_+ > 1$ and positive values of x_m if $n_-/n_+ < 1$. The case where $n_-/n_+ > 1$ or $x_m < 0$ is the case of the salts of inorganic ions: LiCl, KCl, NaCl, KBr, and RbBr. This means that the steepness of the voltage depen-

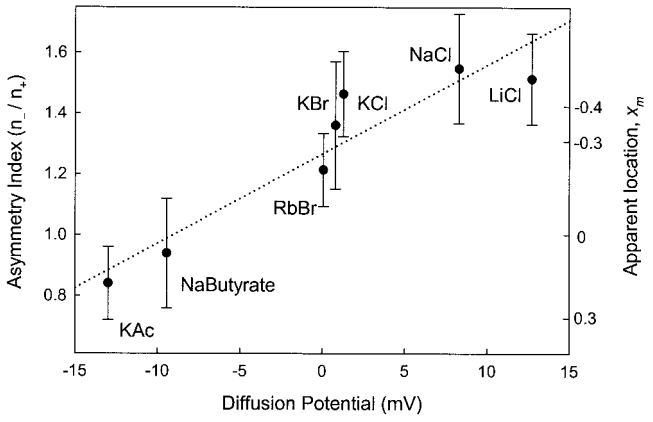

FIGURE 6 Correlation between the calculated diffusion potential of ions flowing through VDAC channels, V_{dif}, and an experimental index of asymmetry in the presence of a 10-fold activity ratio for different salts. The linear regression is shown by the dotted line, and the Pearson correlation coefficient is $r^2 = 0.885$. Data for n_+ and n_- were taken from Table 2 in Zizi et al. (1998). From Eq. 6 or 11, one can get the relationship of the apparent location x_m with this asymmetry index as $n_-/n_+ \propto 1 - 2x_m$. V_{dif} was calculated from the usual expression (See, e.g., Zambrowicz and Colombini, 1993).

dence is greater for $V < V_{max}$ than for $V > V_{max}$. See in Fig. 3 the best-fit values of x_m for KBr ($x_m = -0.3$) and NaCl ($x_m = -0.4$). For the salts of the organic anions, NaButyrate and KAcetate, the probability curve exhibits an asymmetry of opposite sign because $n_-/n_+ < 1$ (i.e., $x_m > 0$).

Let us consider the possible underlying reason for the salt dependence of the sign of the asymmetry index of channel gating. An obvious candidate for the property of the salt that could account for the results is the relative mobility of the cation and anion. The difference in mobility generates a diffusion potential V_{dif}. This is the reason why we considered the correlation between the diffusion potential values calculated for different salts and the corresponding values of an experimental asymmetry index (Fig. 6). There is a clear correlation between these two quantities: higher n_-/n_+ corresponds to higher V_{dif} or, in the context of our model, a higher V_{dif} corresponds to a more negative value of x_m. Because a negative value of x_m corresponds to a location of the mobile charge in the *trans*-half of the channel, Fig. 6 indicates that a higher V_{dif} corresponds to an apparent location of the mobile domain closer to *trans*-entrance. This finding would require that the mobile charge have some mobility in the open state uncoupled to the gating process. Further, this motion must not result in appreciable changes in channel conductivity. The open state does generate a substantial level of current noise (Rostovtseva and Bezrukov, 1998) that might be a manifestation of this motion. Mechanistically, if the diffusion potential is positive (as in the case of the inorganic ions) then its field pushes the mobile charges closer to the *trans* entrance. Thus, the model naturally links the ability of the salt gradient to shift the peak probability to the generation of an asymmetrical voltage dependence of the probability for the two gating processes.

Similarly, a negative V_{dif}, which pushes the mobile domain closer to the *cis*-entrance, should result in a probability curve exhibiting an opposite asymmetry. Just such behavior was observed in solutions of organic ions (NaButyrate and KAcetate). The best fit for the KAcetate probability data (not shown) gave $x_m = +0.3$.

An analogous reasoning can also explain the difference in VDAC gating in charged and neutral lipid membranes. In the case of neutral phospholipids, there are no external electrostatic effects, due to the net charge of the lipid, on the mobile charges of the channel, hence their location is influenced only by intrinsic interactions. Assuming the latter effects cause the apparent mobile charge, q_m, to be shifted from the channel midpoint, then asymmetrical gating would be the result. However, in the presence of charged membranes (soybean phospholipid membrane) the lipid headgroups from both surfaces interact with the mobile charges in opposite directions, causing the channel midpoint to be the energetically favorable position for the mobile charge, q_m. Therefore, the gating processes are expected to be symmetrical in this case.

We have associated the parameter x_m (and consequently the asymmetry index n_-/n_+) with the location of the mobile charge within the channel. However, as noted above, it may have a more general meaning: describing the interaction of the voltage sensor with the applied voltage. Therefore, the changes in x_m may not be the result of the motion of the mobile charged domain but the result of changes in the dielectric environment felt by these charges.

Minor structural charge displacements were also proposed recently (Rostovtseva et al., 2000) to explain cooperativity phenomena in VDAC following changes in pH. These authors concluded that these subtle cooperative structural changes may allow proteins to adapt to changes in their environment. In our model, these changes would be a channel's adaptive response to metabolic fluxes of charged substances with different mobilities.

The gating at high voltages

Let us now consider in detail VDAC gating under high applied voltage. The experimental data (Zizi et al., 1998) manifest that the steepness of the probability curve at relatively small voltages is lower than the same at high voltages and the transition from low to high steepness occurs at higher voltage in concentrated solutions. This difference is more clearly seen in a semi-logarithmic plot of the data. Figure 7 shows the same data plotted in Fig. 2 by using a logarithmic scale for probability.

From these data, it is obvious that the apparent mobile charge (and hence, the mobile sensor also) is not the same at low and high applied voltages, but consists of two parts

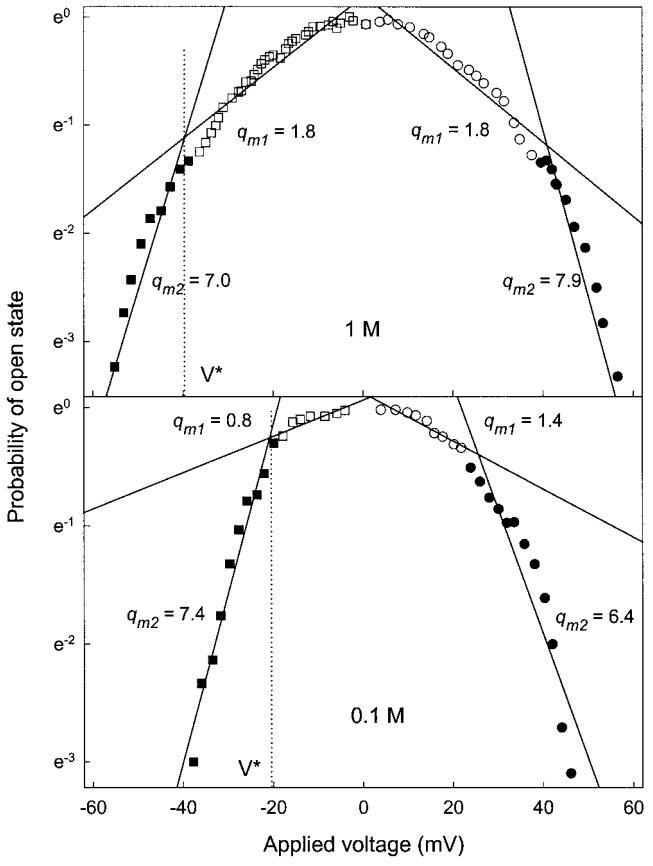

FIGURE 7 Representation of Fig. 2 on a semi-logarithmic scale. The experimental data have been divided into four data subsets shown by different symbols, and regression lines are drawn for each one of them. The values of q_{m1} and q_{m2} shown in the panel have been obtained from these regression analyses. Voltage threshold values are shown in both plots. See main text for details.

at least (we denote them here q_{m1} and q_{m2}), which have to overcome different energetic barriers ΔE^{m1}_{other} and ΔE^{m2}_{other} in the channel-closing process. Moreover, $\Delta E^{m2}_{other} > \Delta E^{m1}_{other}$, and $q_{m2} > q_{m1}$. Therefore, VDAC gating can thus be rationalized in the following way: at low voltages, the motion of q_{m1} is far more likely because the energy barrier for the motion of q_{m2} is higher. Thus, channels gate with shallower voltage dependence. However, because the effective energetic barrier $\Delta E^{m2}_{other} - (x_m + 1)q_{m2}|V|/2$ decreases with the increase of voltage, when the applied voltage reaches the threshold value $|V^*| \approx 2\Delta E^{m2}_{other}/q_{m2}(x_m + 1)$, the mobile charge, q_{m2}, also takes part in channel closure. From Fig. 7, it becomes apparent that the average value of steepness at low and high voltages is greater than the fitted value for q_m obtained from our model, and it is closer to reported values of the voltage sensor charge in the literature (~5–6) (Peng et al., 1992).

Then a question arises: why do the barriers depend on the concentration of the surrounding solution? An answer can be given within the framework of the present approach. As mentioned above, E^{m2}_{other} contains the term $\alpha q_f/C < 0$ (see Eqs. 9 and 10). Therefore, the voltage needed to compensate for the energy barrier scales inversely with salt activity ($|V^*| \approx$ constant $- 1/C$), which explains the higher voltage needed to cause the second set of charges to move in concentrated salt solutions. Therefore, this discussion on gating at high voltages in the framework of our approach supports the main role of electrostatics in the gating process.

CONCLUSIONS

VDAC gating in the presence of a salt gradient has been analyzed by assuming that the channel occupies conformational states based on their respective electrostatic energies. The voltage dependence of VDAC gating, both in the presence and in the absence of a salt activity gradient, was explained just by invoking electrostatic interactions. A model describing this energy in the main VDAC states (open, *trans*-closed, and *cis*-closed) has been developed. On the basis of the model, we have considered the redistribution of the channels into the various states upon external influences. According to this model, shifts along the voltage axis of the open probability curve of VDAC arise from differences in the energy levels of the *trans*- and *cis*-closed states that exist at zero transmembrane voltage. This difference is, in turn, the result of different electrostatic interactions of the voltage sensor with channel fixed charge within the pore, when the former is on the *cis* side of the membrane and on the *trans* side. The theory describes satisfactorily the experimental data (Zizi et al. 1998) and explains the nature of the probability curve and the difference in curve asymmetry in different salts. The asymmetry of the probability curve was connected with the apparent location of the VDAC voltage sensor in the open state. By analyzing published experimental data, we concluded that this apparent location is influenced by the diffusion potential. It was also shown that VDAC gating at high voltage is better described by assuming that the mobile charge consists of two parts that have to overcome different energetic barriers in the channel-closing process. The current model does not negate the concept of kinetic energy transfer between the movement of the ions in solution down their gradient and the sensor, resulting in a shift in the open probability curve. It provides an alternative explanation, and, indeed, both processes may be simultaneously influencing the gating of VDAC.

V.L. thanks financial support from Generalitat Valenciana and Universitat Jaume I through a grant for invited scientists. V.A. thanks financial support from Fundació Caixa-Castelló (project P1B98-12) and from DGICYT (project P1-1B2001-20). M.C. is grateful for the support of the National Science Foundation (MCB-9816788).

REFERENCES

Colombini, M. 1979. A candidate for the permeability pathway of the outer mitochondrial membrane. *Nature.* 279:643–645.

Colombini, M. 1987. Characterization of channels isolated from plant mitochondria. *Methods Enzymol.* 148:465–475.

Colombini, M., E. Blachly-Dyson, and M. Forte. 1996. VDAC, a channel in the outer mitochondrial membrane. *In* Ion Channels, Vol. 4. T. Narahashi, editor. Plenum Publishing, New York. 169–202.

Ermishkin, L., and T. Mirzabekov. 1990. Redistribution of the electric field within the pore contributes to the voltage dependence of mitochondrial porin channel. *Biochim. Biophys. Acta.* 1021:161–168.

Levadny, V., and V. M. Aguilella. 2001. Reversal potential of a wide ion channel. Non-uniform charge distribution effects. *J. Phys. Chem. B.* 105:9902–9908.

Mannella, C. 1982. Structure of the outer mitochondrial membrane: ordered arrays of pore-like subunits in the outer membrane fractions from *Neurospora crassa* mitochondria. *J. Cell Biol.* 94:680–687.

Peng, S., E. Blachly-Dyson, M. Forte, and M. Colombini. 1992. Large scale rearrangement of protein domains is associated with voltage gating of the VDAC channel. *Biophys. J.* 62:123–135.

Rostovtseva, T. K., and S. M. Bezrukov. 1998. ATP transport through a single mitochondrial channel, VDAC, studied by current fluctuation analysis. *Biophys. J.* 74:2365–2373.

Rostovtseva, T. K., T. Liu, M. Colombini, V. A. Parsegian, and S. M. Bezrukov. 2000. Positive cooperativity without domains or subunits in a monomeric membrane channel. *Proc. Natl. Acad. Sci. U.S.A.* 97: 7819–7822.

Song, J., C. Midson, E. Blachly-Dyson, M. Forte, and M. Colombini. 1998. Large scale rearrangement of protein domains is associated with voltage gating of the VDAC channel. *Biophys. J.* 74:2926–2944.

Sørensen, T. S., and J. Koefoed. 1974. Electrokinetic effects in charged capillary tubes. *J. Chem. Soc. Faraday Trans. II.* 70:665–675.

Thomas, L., E. Blachly-Dyson, M. Colombini, and M. Forte. 1993. Mapping of residues forming the voltage sensor of the voltage-dependent anion-selective channel. *Proc. Natl. Acad. Sci. U.S.A.* 90:5446–5449.

Zambrowicz, E. B., and M. Colombini. 1993. Zero-current potentials in a large membrane channel: a simple theory accounts for complex behavior. *Biophys. J.* 65:1093–1100.

Zizi, M., C. Bird, R. Boxus, and M. Colombini. 1998. The voltage-gating process of the voltage-dependent anion channel is sensitive to ion flow. *Biophys. J.* 75:704–713.